Electromagnetics Laboratory Report Series

Espoo, April 2004 REPORT 434

SOLVING ELECTROMAGNETIC BOUNDARY PROBLEMS WITH EQUIVALENCE METHODS

Jari J. Hänninen

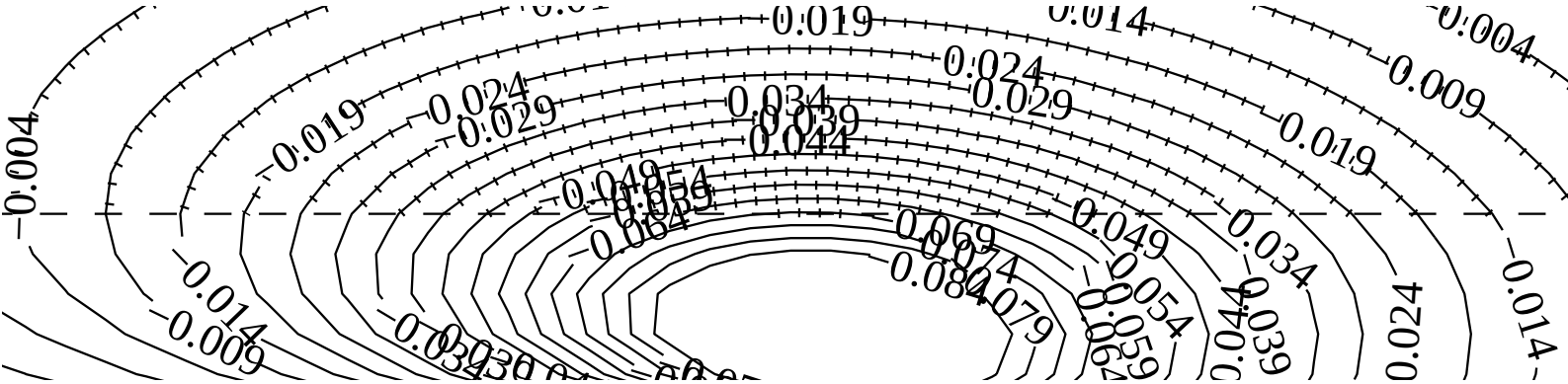

TEKNILLINEN KORKEAKOULU
TEKNISKA HÖGSKOLAN
HELSINKI UNIVERSITY OF TECHNOLOGY
TECHNISCHE UNIVERSITÄT HELSINKI
UNIVERSITE DE TECHNOLOGIE D'HELSINKI

Electromagnetics Laboratory Report Series
Espoo, April 2004 REPORT 434

SOLVING ELECTROMAGNETIC BOUNDARY PROBLEMS WITH EQUIVALENCE METHODS

Jari J. Hänninen

Dissertation for the degree of Doctor of Science in Technology to be presented with due permission of the Department of Electrical and Communications Engineering, Helsinki University of Technology, for public examination and debate in Auditorium S4 at Helsinki University of Technology (Espoo, Finland) on the 7th of May, 2004, at 12 noon.

Helsinki University of Technology
Department of Electrical and Communications Engineering
Electromagnetics Laboratory

Distribution:
Helsinki University of Technology
Electromagnetics Laboratory
P.O. Box 3000
FIN-02015 HUT
Tel. +358 9 451 2264
Fax +358 9 451 2267

ISBN 951-22-7080-3
ISSN 1456-632X

Picaset Oy
Helsinki 2004

Abstract

A basic problem in electromagnetics involves solving the Maxwell equations in a non-empty space, i.e. in a space with interfaces or boundaries. In this dissertation the wanted electromagnetic fields are searched via equivalence methods: a full electromagnetic problem is transformed to a simpler solvable form, or the solution is an equivalent source, or both. The chosen transformations result to two slightly different transmission line formulations or to Kelvin inversion (inversion in a sphere). The equivalent source is typically an image source. The included cases are 1) a planar multilayer chiral structure, 2) a conducting earth under a current source, 3) a sphere in an isotropic or bi-isotropic space, and 4) three types of anisotropic half-space–planar boundary or half-space problems. The first two cases (three papers) are time-dependent problems and the latter two (four papers) statics or quasi-statics. In each case the solution methodology is presented, the solutions are written, and the implications and limitations are discussed.

Keywords:

equivalence method — equivalent source — electromagnetic image principle — Kelvin inversion — bi-isotropic medium — anisotropic medium — exact image theory (EIT) — geomagnetically induced currents (GIC) — transmission line — electrostatics

O glaube, mein Herz, o glaube: Es geht dir nichts verloren!
Dein ist, ja dein, was du gesehnt!
Dein, was du geliebt, was du gestritten!
O glaube: Du wardst nicht umsonst geboren!
Hast nicht umsonst gelebt, gelitten!

Gustav Mahler
in the fifth movement of his Second Symphony
toisen sinfoniansa viidennessä osassa

Thanks

For ideas and fruitful collaboration: Professor Ismo V. Lindell, supervisor of the thesis;
Professor Keijo Nikoskinen, my trusted colleague.
For swiftness: Docent Esko Eloranta and D.Sc.(Tech) Murat Ermutlu,
pre-examiners of the thesis.
For employment and funding: Professor Ari Sihvola, Head of Laboratory;
Graduate School of Applied Electromagnetics.
For assistance in practical matters: Katrina Nykänen, Secretary of Laboratory.
For enduring my jokes: M.Sc.(Tech) Sami Ilvonen, my friend sharing the workroom.
For cheerful moments: my fellow post-graduates; my dear friends.
For participation: the rest of the Laboratory personnel;
other involved persons not yet mentioned.
For life: my beloved parents Paavo and Liisa.

Jari J. Hänninen
Espoo, Finland, 16th April 2004

Kiitokset

Ideoista ja tuloksekkaasta yhteistyöstä: väitöskirjatyön valvoja professori Ismo V. Lindell;
luottokollegani professori Keijo Nikoskinen.
Joutuisuudesta: väitöskirjan esitarkastajat dosentti Esko Eloranta ja TkT Murat Ermutlu.
Työsuhteesta ja rahoituksesta: laboratorion johtaja professori Ari Sihvola;
sovelletun sähkömagnetiikan tutkijakoulu.
Käytännön asiain hoidosta: laboratorion sihteeri Katrina Nykänen.
Vitsieni kestämisestä: työhuoneystäväni DI Sami Ilvonen.
Hilpeistä hetkistä: jatko-opiskelutoverini; armaat ystäväni.
Osallistumisesta: loput virkaveljeni laboratoriossa;
vielä mainitsemattomat muut mukanaolleet.
Elämästä: rakkaat vanhempani Paavo ja Liisa.

Jari J. Hänninen
Espoossa 16. huhtikuuta 2004

List of publications

[P1] Oksanen, M.I., Hänninen, J. & Tretyakov, S.A. "Vector circuit method for calculating reflection and transmission of electromagnetic waves in multilayer chiral structures". *IEE Proceedings H, Microwaves, Antennas and Propagation,* **138**(1991)6, p. 513–520.

[P2] Lindell, I.V. & Hänninen, J.J. "Static image principle for the sphere in isotropic or bi-isotropic space". *Radio Science,* **35**(2000)3, p. 653–660.

[P3] Lindell, I.V., Hänninen, J.J. & Pirjola, R. "Wait's complex-image principle generalized to arbitrary sources". *IEEE Transactions on Antennas and Propagation,* **48**(2000)10, p. 1618–1624.

[P4] Hänninen, J.J., Pirjola, R.J. & Lindell, I.V. "Application of the EIT to studies of ground effects of space weather". *Geophysical Journal International,* **151**(2002)-, p. 534–542.

[P5] Lindell, I.V., Hänninen, J.J. & Nikoskinen, K.I. "Electrostatic image theory for an anisotropic boundary". *IEE Proceedings—Science, Measurement & Technology,* accepted for publication.

[P6] Hänninen, J.J., Lindell, I.V. & Nikoskinen, K.I. "Electrostatic image theory for an anisotropic boundary of an anisotropic half-space". *Progress in Electromagnetics Research,* **47**(2004)-, p. 235–262.

[P7] Hänninen, J.J., Nikoskinen, K.I. & Lindell, I.V. *Electrostatic image theory for two anisotropic half-spaces.* (Electromagnetics Laboratory Report Series, Report 428). Espoo, Finland 2004: Helsinki University of Technology, Electromagnetics Laboratory. (Submitted in shorter form to *Electrical Engineering (Archiv für Elektrotechnik).*)

Contribution of the author

In all the papers the first author was responsible for the manuscript.

The papers [P4], [P6], and [P7] were mainly done by the author of the thesis; this included developing the theory, presenting it, and verifying the results.

Papers [P1]–[P3] and [P5] were the result of collaboration of the authors; the thesis author took especially care of the numerical verifications (where applicable).

1 Introduction

Take an empty universe (in the classical sense), set a charge distribution "somewhere," and express the density and time-dependence of that charge distribution as a function of position and time. Because electromagnetic field theory has long since been equipped with Green functions for free space, it should be straightforward to calculate the fields emanating from this source, be the source truly time-varying or static.

In principle the sketched process could be applied to a non-empty universe like ours. Instead of having free space we now have boundaries (changes in material parameters), but we could try to construct a Green function—the field of a point source—for the geometry involved and determine the electromagnetic field for all possible sources by integration. The bad news is that it is extremely difficult to construct Green functions for general boundary problems. Some detour is necessary...

An 'equivalence method' in electromagnetics is an indirect method with which it is possible to obtain a solution to the original electromagnetic problem which may otherwise be difficult or impossible to solve. As will be seen later, the equivalence may mean utilising some mathematical apparatus to write the equations of the problem in a new "language" (physical space–Maxwell equations vs. Fourier-space–transmission line equations), or it may mean that an obtained result (e.g., a reflection image source), after proper application, gives correct electromagnetic fields in (some part of) the physical space under study. These classes may also be combined, giving two instances or levels of equivalence inside one problem.

This Summary first collects some common electromagnetic formulas. The seven included papers are then scrutinised in Section 5 to show various equivalence methods in action, both on the problem-solving level and on the result level. The aim is to give a general view of equivalence methods and also to discuss some aspects of the results, though this is mainly covered by the papers themselves.

Among solution-level equivalence methods can be counted the use of different transmission line analogies [P1] and [P5]–[P7], and Kelvin inversion [P2]. On the result level we see reflection or transmission coefficients in [P1], or equivalent sources (images) in [P2]–[P7]. In [P1] we have the plane wave excitation disguised as an equivalent source!

2 Electromagnetic formulation

2.1 Maxwell equations

The classical electromagnetic field theory—or electrodynamics, as it is also called—is built upon the four *Maxwell equations* [D1, (3.1)–(3.4)]

$$\nabla \times \bar{\mathbf{E}}(\bar{\mathbf{r}}, t) = -\frac{\partial}{\partial t}\bar{\mathbf{B}}(\bar{\mathbf{r}}, t) \qquad \text{(Faraday's law)}, \tag{D1}$$

$$\nabla \times \bar{\mathbf{H}}(\bar{\mathbf{r}}, t) = \bar{\mathbf{J}}(\bar{\mathbf{r}}, t) + \frac{\partial}{\partial t}\bar{\mathbf{D}}(\bar{\mathbf{r}}, t) \qquad \text{(Ampère's law)}, \tag{D2}$$

$$\nabla \cdot \bar{\mathbf{D}}(\bar{\mathbf{r}}, t) = \varrho(\bar{\mathbf{r}}, t) \qquad \text{(Gauss' law), and} \tag{D3}$$

$$\nabla \cdot \bar{\mathbf{B}}(\bar{\mathbf{r}}, t) = 0. \tag{D4}$$

Here $\bar{\mathbf{E}}(\bar{\mathbf{r}}, t)$ is the electric field (strength), $\bar{\mathbf{D}}(\bar{\mathbf{r}}, t)$ is the electric flux density (or electric displacement), $\bar{\mathbf{H}}(\bar{\mathbf{r}}, t)$ is the magnetic field (strength), and $\bar{\mathbf{B}}(\bar{\mathbf{r}}, t)$ is the magnetic flux density (or magnetic induction). The sources of the electromagnetic fields are the current

density $\bar{\mathbf{J}}(\bar{\mathbf{r}},t)$ and the electric charge density $\varrho(\bar{\mathbf{r}},t)$. Equation (D4) is usually left unnamed because free magnetic charges (monopoles) have not been observed (although Dirac's theory [D2] favours their existence). However, it is occasionally useful to symmetrize the right-hand sides of the equations by adding a magnetic charge density $\varrho_{\mathrm{m}}(\bar{\mathbf{r}},t)$ to (D4) and a corresponding negative magnetic current density $-\bar{\mathbf{J}}_{\mathrm{m}}(\bar{\mathbf{r}},t)$ to (D1).

We can apply the Fourier transformation pair

$$F(\bar{\mathbf{r}},\omega)=\int_{-\infty}^{\infty} f(\bar{\mathbf{r}},t)e^{-j\omega t}\,dt \quad \leftrightarrow \quad f(\bar{\mathbf{r}},t)=\frac{1}{2\pi}\int_{-\infty}^{\infty} F(\bar{\mathbf{r}},\omega)e^{j\omega t}\,d\omega \tag{D5}$$

to Maxwell equations to obtain equations without explicit time derivatives (magnetic charges again omitted):

$$\nabla\times\bar{\mathbf{E}}(\bar{\mathbf{r}},\omega)=-j\omega\bar{\mathbf{B}}(\bar{\mathbf{r}},\omega), \tag{D6}$$
$$\nabla\times\bar{\mathbf{H}}(\bar{\mathbf{r}},\omega)=\bar{\mathbf{J}}(\bar{\mathbf{r}},\omega)+j\omega\bar{\mathbf{D}}(\bar{\mathbf{r}},\omega), \tag{D7}$$
$$\nabla\cdot\bar{\mathbf{D}}(\bar{\mathbf{r}},\omega)=\varrho(\bar{\mathbf{r}},\omega), \tag{D8}$$
$$\nabla\cdot\bar{\mathbf{B}}(\bar{\mathbf{r}},\omega)=0. \tag{D9}$$

All quantities are now complex. By the left-hand equation of (D5) we see that $F(\bar{\mathbf{r}},-\omega)=F^{*}(\bar{\mathbf{r}},\omega)$ because physical time-dependent fields are real.

If we assume that the electromagnetic sources (and thus the fields) have a single-frequency sinusoidal time dependence, a function $f(\bar{\mathbf{r}},t)$ is related to the complex function $F(\bar{\mathbf{r}})$ by

$$f(\bar{\mathbf{r}},t)=\Re\left\{F(\bar{\mathbf{r}})e^{j\omega t}\right\}, \tag{D10}$$

where $F(\bar{\mathbf{r}})$ is a Fourier-transformed quantity (phasor, complex vector) without the negative frequencies. In this *time-harmonic* case we usually write the Maxwell equations in short form, without the argument ω, i.e. $\nabla\times\bar{\mathbf{E}}(\bar{\mathbf{r}})=-j\omega\bar{\mathbf{B}}(\bar{\mathbf{r}})$, etc. From now on we employ the short form.—In papers [P1], [P3] and [P4] time-harmonic fields are discussed.

It is easy to see from equations (D7) and (D8) that $\nabla\cdot\bar{\mathbf{J}}(\bar{\mathbf{r}})=-j\omega\varrho(\bar{\mathbf{r}})$, so we do not need to use (D8) explicitly when solving time-harmonic problems. Likewise, taking the divergence of equation (D6) gives us equation (D9) directly.

Electric and magnetic quantities decouple if there is no time dependence, $\partial f(\bar{\mathbf{r}},t)/\partial t\equiv 0$ or $\omega\equiv 0$. We then get electrostatics,

$$\nabla\times\bar{\mathbf{E}}(\bar{\mathbf{r}})=\bar{\mathbf{0}}, \tag{D11}$$
$$\nabla\cdot\bar{\mathbf{D}}(\bar{\mathbf{r}})=\varrho(\bar{\mathbf{r}}), \tag{D12}$$

or magnetostatics

$$\nabla\times\bar{\mathbf{H}}(\bar{\mathbf{r}})=\bar{\mathbf{J}}(\bar{\mathbf{r}}), \tag{D13}$$
$$\nabla\cdot\bar{\mathbf{B}}(\bar{\mathbf{r}})=0. \tag{D14}$$

It should be observed that $\nabla\cdot\bar{\mathbf{J}}(\bar{\mathbf{r}})=0$, which means that there is no accumulation of charge (in time) anywhere. Under static conditions all quantities are real. Also, in electrostatics we have the possibility of using electric potential $\phi(\bar{\mathbf{r}})$, which gives the electric field via $\bar{\mathbf{E}}(\bar{\mathbf{r}})=-\nabla\phi(\bar{\mathbf{r}})$.—Papers [P2] and [P5]–[P7] handle statics or quasistatics.

2.2 Constitutive relations

In the Maxwell equations we have 12 unknowns and only six independent equations—(D3) and (D4) are obtainable from (D2) and (D1), respectively. So, we need to relate the field vectors $\bar{\mathbf{E}}$, $\bar{\mathbf{B}}$, $\bar{\mathbf{H}}$, and $\bar{\mathbf{D}}$ with additional constraints to solve field problems. This is done by taking the effects of material media into account with *constitutive relations*. For example, in a linear *bianisotropic medium* we have [D1, p. 54]

$$\bar{\mathbf{D}} = \bar{\bar{\boldsymbol{\epsilon}}} \cdot \bar{\mathbf{E}} + \bar{\bar{\boldsymbol{\xi}}} \cdot \bar{\mathbf{H}}, \tag{D15}$$

$$\bar{\mathbf{B}} = \bar{\bar{\boldsymbol{\zeta}}} \cdot \bar{\mathbf{E}} + \bar{\bar{\boldsymbol{\mu}}} \cdot \bar{\mathbf{H}}. \tag{D16}$$

The exact physical behaviour of a medium is hidden inside the dyadic medium parameters $\bar{\bar{\boldsymbol{\epsilon}}}$ (permittivity), $\bar{\bar{\boldsymbol{\xi}}}$, $\bar{\bar{\boldsymbol{\zeta}}}$ (magnetoelectric dyadics), and $\bar{\bar{\boldsymbol{\mu}}}$ (permeability). (Here the medium is assumed to be local and non-dispersive.) We can also relate the electric field and current density via *Ohm's law:*

$$\bar{\mathbf{J}} = \bar{\bar{\boldsymbol{\sigma}}} \cdot \bar{\mathbf{E}}, \tag{D17}$$

where $\bar{\bar{\boldsymbol{\sigma}}}$ is the conductivity dyadic.

If the medium dyadics are multiples of the unit dyadic $\bar{\bar{\mathbf{I}}}$, i.e. $\bar{\bar{\boldsymbol{\epsilon}}} = \epsilon\bar{\bar{\mathbf{I}}}$, $\bar{\bar{\boldsymbol{\xi}}} = \xi\bar{\bar{\mathbf{I}}}$, $\bar{\bar{\boldsymbol{\zeta}}} = \zeta\bar{\bar{\mathbf{I}}}$, and $\bar{\bar{\boldsymbol{\mu}}} = \mu\bar{\bar{\mathbf{I}}}$, the medium is said to be *bi-isotropic.* This kind of medium is encountered in paper [P2]. If we simplify the material even further, we get an isotropic *chiral medium* having $\xi = -j\kappa\sqrt{\mu_0\epsilon_0}$ and $\zeta = j\kappa\sqrt{\mu_0\epsilon_0}$. Chiral materials are discussed in paper [P1]. If the chirality parameter κ is zero, we end up with an "ordinary" *isotropic medium* with the constitutive equations

$$\bar{\mathbf{D}} = \epsilon\,\bar{\mathbf{E}}, \tag{D18}$$

$$\bar{\mathbf{B}} = \mu\,\bar{\mathbf{H}}. \tag{D19}$$

In free space $\epsilon = \epsilon_0$ and $\mu = \mu_0$. This is the type of medium met in papers [P3], [P4], and [P5].

The bi-isotropic material parameters $\bar{\bar{\boldsymbol{\xi}}}$ and $\bar{\bar{\boldsymbol{\zeta}}}$ are nonzero only under time-varying conditions. In electrostatics we can nevertheless have *anisotropic materials,* described by the relation

$$\bar{\mathbf{D}} = \bar{\bar{\boldsymbol{\epsilon}}} \cdot \bar{\mathbf{E}}. \tag{D20}$$

This is something we look at in papers [P6] and [P7]. Under dynamic conditions the medium relation would look the same but the medium dyadic would not necessarily be symmetric and positive definite, as it is in electrostatics [D3, §13 & §21].

After adding the constitutive relations we have taken one step forward in solving the Maxwell equations. What are needed to finish the process are the interface conditions, which we discuss next.

2.3 Interface conditions

In the previous section we considered media that could be assumed to be *homogeneous* over at least some small region of space. If the medium parameters are discontinuous, for example, there is a planar or spherical surface separating two different dielectrics, the electromagnetic fields will also have discontinuities. These discontinuities can be taken into account with the

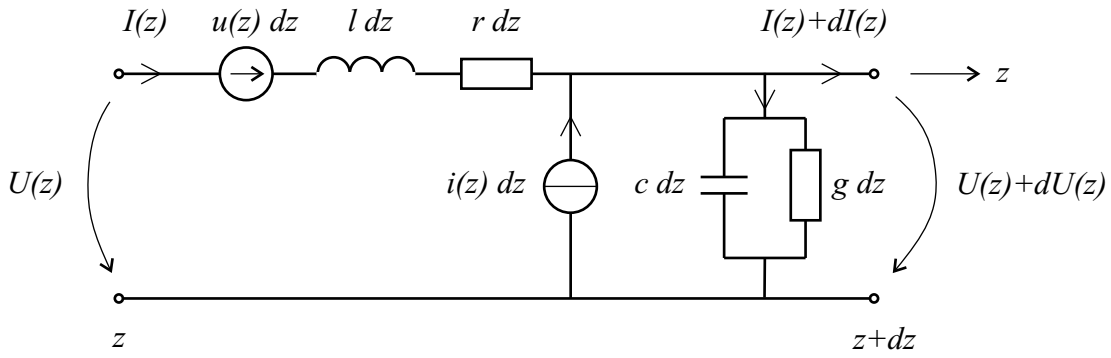

Figure D1: The transmission line model relevant to Section 3.1.

interface conditions [D4, p. 18–29]

$$\bar{\mathbf{n}} \times (\bar{\mathbf{E}}_1 - \bar{\mathbf{E}}_2) = \bar{\mathbf{0}}, \tag{D21}$$
$$\bar{\mathbf{n}} \times (\bar{\mathbf{H}}_1 - \bar{\mathbf{H}}_2) = \bar{\mathbf{J}}_\mathrm{s}, \tag{D22}$$
$$\bar{\mathbf{n}} \cdot (\bar{\mathbf{D}}_1 - \bar{\mathbf{D}}_2) = \varrho_\mathrm{s}, \tag{D23}$$
$$\bar{\mathbf{n}} \cdot (\bar{\mathbf{B}}_1 - \bar{\mathbf{B}}_2) = 0, \tag{D24}$$

where $\bar{\mathbf{n}}$ is the unit normal vector of the interface and it points from medium 2 into medium 1. The field values, the surface charge density ϱ_s and current density $\bar{\mathbf{J}}_\mathrm{s}$ are taken *on* the surface. Simply put, the interface conditions express the continuity of the tangential component of the field strength quantities and the continuity of the normal component of the flux density quantities. (Of course, if there exists surface current or charge, the "continuity" will be a jump discontinuity.)

We talk of *boundary conditions* if the fields on one side of the interface vanish, implying, e.g., $\bar{\mathbf{n}} \times \bar{\mathbf{E}}_1 = 0$ or $\bar{\mathbf{n}} \times \bar{\mathbf{H}}_1 = 0$. These are the cases of perfect electric (PEC) and perfect magnetic conductor (PMC), respectively. In papers [P5] and [P6] we see another boundary condition: the anisotropic impedance boundary.

It perhaps good to remind here that with 'boundary conditions' we may mean the above mentioned field-ending condition, or boundary conditions in the sense they appear in the theory of differential equations, there meaning the equation-supplementing information needed to obtain a unique solution.

Now we have reached the point at which we are able to solve the Maxwell equations—at least in principle. Of course, real engineering problems can be so complicated that exact analytical solutions cannot be obtained, and a suitable numerical method is needed. However, numerical analysis is not discussed here, it being a vast discipline of its own.

3 Solution-level equivalence

Here we look at some methods of translating vector problems into scalar form or transforming geometry in such a way that known solutions can be used to get new ones.

3.1 The transmission line model

We take a length dz of a lossy transmission line, Figure (D1). Using circuit theory we have the two time-harmonic equations

$$U(z) + u(z)\,dz - (j\omega l + r)\,dz - (U(z) + dU(z)) = 0, \tag{D25}$$

$$I(z) - (I(z) + dI(z)) + i(z)\,dz - (j\omega c + g)\,dz \cdot (U(z) + dU(z)) = 0. \tag{D26}$$

After writing out the differentials, i.e. $dI(z) = \partial_z I(z)\,dz$ etc., and neglecting higher order differentials we get the transmission line equation

$$\begin{pmatrix} \partial_z & (j\omega l + r) \\ (j\omega c + g) & \partial_z \end{pmatrix} \begin{pmatrix} U(z) \\ I(z) \end{pmatrix} = \begin{pmatrix} u(z) \\ i(z) \end{pmatrix}. \tag{D27}$$

If we can cast vector equations into scalar form, which has for example been done in papers [P5]–[P7] by using the two-dimensional Fourier transformation, we can use the full set of tools from transmission line theory to determine reflection and transmission coefficients in various geometries.

Paper [P2] has a different approach: there a vector circuit has been used. For further reference the paper itself should be studied.

3.2 Affine transformation

In paper [P6] the image source is constructed via the transmission line equivalence. The result of [P5] at our disposal, we could have used *affine transformation* to turn the isotropic permittivity of the upper half-space into an anisotropic one, giving essentially the same end result as in [P6]. However, the derivation is quite long, and though in paper [P6, (53)] (and [P7]) an affine transformation is being used, it takes place deep inside the formulation. Here a from-the-start affine transformation method is outlined.

We start with the anisotropic problem and look for an affine transformation that transforms the anisotropic half-space into an isotropic one. This process gives us a dictionary for moving back and forth between the two spaces. Then, using the existing results in [P5], we could find the image source of a point source above an anisotropic impedance surface and transform the image, the boundary, and the geometry into our anisotropic space. It should be noted that for practical purposes we should apply the affine transformation twice—first to transform the anisotropic case isotropic ('forward') and then back ('inverse'). Here we assume, for the sake of clarity, that the first transformation has been carried out already.

3.2.1 Transforming the equations

We use the electrostatic Maxwell equations (D11) and (D12), and the constitutive relation (D20). The general permittivity dyadic $\bar{\bar{\boldsymbol{\epsilon}}}_{\mathrm{r}}$ is, of course, symmetric and positive definite.

From now on we *denote quantities of the isotropic case with primes* (and the anisotropic case without). The Cartesian unit vectors $(\bar{\mathbf{u}}_x, \bar{\mathbf{u}}_y, \bar{\mathbf{u}}_z)$ coincide with the isotropic geometry but are unprimed because they form the invariant coordinate framework. (Dyadic notation would allow us to avoid using coordinates, but illustrating the affine transformation without any coordinate system would be difficult.)

First we seek the transformation $\nabla \leftrightarrow \nabla'$. Utilising (D12) and requiring the Maxwell

equations to hold in both spaces we get

$$\begin{aligned} & \epsilon_0 \nabla \cdot \bar{\bar{\epsilon}}_\mathrm{r} \cdot \bar{\mathbf{E}}(\bar{\mathbf{r}}) = \varrho(\bar{\mathbf{r}}) \\ \Leftrightarrow \quad & \epsilon_0 \nabla \cdot \bar{\bar{\epsilon}}_\mathrm{r}^{1/2} \cdot \bar{\bar{\epsilon}}_\mathrm{r}^{1/2} \cdot \bar{\mathbf{E}}(\bar{\mathbf{r}}) = \varrho(\bar{\mathbf{r}}) \\ \Leftrightarrow \quad & \epsilon_0 (\bar{\bar{\epsilon}}_\mathrm{r}^{1/2} \cdot \nabla) \cdot (\bar{\bar{\epsilon}}_\mathrm{r}^{1/2} \cdot \bar{\mathbf{E}}(\bar{\mathbf{r}})) = \varrho(\bar{\mathbf{r}}) \\ \Leftrightarrow \quad & \epsilon_0 \nabla' \cdot \bar{\mathbf{E}}'(\bar{\mathbf{r}}') = \varrho'(\bar{\mathbf{r}}') \end{aligned} \tag{D28}$$

if we identify

$$\nabla' = \bar{\bar{\epsilon}}_\mathrm{r}^{1/2} \cdot \nabla \quad \leftrightarrow \quad \nabla = \bar{\bar{\epsilon}}_\mathrm{r}^{-1/2} \cdot \nabla', \tag{D29}$$

$$\bar{\mathbf{E}}'(\bar{\mathbf{r}}') = \bar{\bar{\epsilon}}_\mathrm{r}^{1/2} \cdot \bar{\mathbf{E}}(\bar{\mathbf{r}}) \quad \leftrightarrow \quad \bar{\mathbf{E}}(\bar{\mathbf{r}}) = \bar{\bar{\epsilon}}_\mathrm{r}^{-1/2} \cdot \bar{\mathbf{E}}'(\bar{\mathbf{r}}'). \tag{D30}$$

From (D28) it is immediately seen that we have got an isotropic medium in the primed space:

$$\bar{\mathbf{D}}'(\bar{\mathbf{r}}') = \epsilon_0 \bar{\mathbf{E}}'(\bar{\mathbf{r}}'), \tag{D31}$$

$$\nabla' \cdot \bar{\mathbf{D}}'(\bar{\mathbf{r}}') = \varrho'(\bar{\mathbf{r}}'). \tag{D32}$$

The charge density has, of course, a different-looking expression in each space but otherwise it is an invariant, i.e. $\varrho(\bar{\mathbf{r}}) = \varrho'(\bar{\mathbf{r}}')$. See below for the further discussion of the sources.

Transformation $\bar{\mathbf{r}} \leftrightarrow \bar{\mathbf{r}}'$ is obtained from (D29) and the identity $\bar{\bar{\mathbf{I}}} = \nabla \bar{\mathbf{r}} = \nabla' \bar{\mathbf{r}}'$:

$$\bar{\bar{\mathbf{I}}} = \nabla' \bar{\mathbf{r}}' = (\bar{\bar{\epsilon}}_\mathrm{r}^{1/2} \cdot \nabla) \bar{\mathbf{r}}' = \nabla (\bar{\bar{\epsilon}}_\mathrm{r}^{1/2} \cdot \bar{\mathbf{r}}') = \nabla \bar{\mathbf{r}}. \tag{D33}$$

This gives the pair (which could have been used *to define* the affine transformation)

$$\bar{\mathbf{r}}' = \bar{\bar{\epsilon}}_\mathrm{r}^{-1/2} \cdot \bar{\mathbf{r}} \quad \leftrightarrow \quad \bar{\mathbf{r}} = \bar{\bar{\epsilon}}_\mathrm{r}^{1/2} \cdot \bar{\mathbf{r}}'. \tag{D34}$$

Finally, before proceeding to the handling of boundary conditions, let us verify the previous results by applying the identity $(\bar{\bar{\mathbf{A}}} \cdot \bar{\mathbf{a}}) \times (\bar{\bar{\mathbf{A}}} \cdot \bar{\mathbf{b}}) = \bar{\bar{\mathbf{A}}}^{(2)} \cdot (\bar{\mathbf{a}} \times \bar{\mathbf{b}}) = \frac{1}{2} (\bar{\bar{\mathbf{A}}} \mathbin{\overset{\times}{\times}} \bar{\bar{\mathbf{A}}}) \cdot (\bar{\mathbf{a}} \times \bar{\mathbf{b}})$ to (D11), giving us

$$\nabla \times \bar{\mathbf{E}}(\bar{\mathbf{r}}) = (\bar{\bar{\epsilon}}_\mathrm{r}^{-1/2} \cdot \nabla') \times (\bar{\bar{\epsilon}}_\mathrm{r}^{-1/2} \cdot \bar{\mathbf{E}}'(\bar{\mathbf{r}}')) = (\bar{\bar{\epsilon}}_\mathrm{r}^{-1/2})^{(2)} \cdot (\nabla' \times \bar{\mathbf{E}}'(\bar{\mathbf{r}}')) = \bar{\mathbf{0}} \quad \Leftrightarrow \quad \nabla' \times \bar{\mathbf{E}}'(\bar{\mathbf{r}}') = \bar{\mathbf{0}}. \tag{D35}$$

So, with the chosen affine transformation the Maxwell equations remain intact.

3.2.2 Transforming the sources and boundary conditions

The impedance boundary condition of the anisotropic surface $z = 0$ of the *isotropic* half-space $z > 0$ is

$$\bar{\mathbf{n}}' \cdot \bar{\mathbf{D}}'(\bar{\boldsymbol{\rho}}') = -\nabla_\mathrm{t}' \cdot \bar{\boldsymbol{\Psi}}_\mathrm{s}'(\bar{\boldsymbol{\rho}}') = -\epsilon_0 \nabla_\mathrm{t}' \cdot \bar{\bar{\boldsymbol{\zeta}}}_\mathrm{r}' \cdot \bar{\mathbf{E}}_\mathrm{t}'(\bar{\boldsymbol{\rho}}'). \tag{D36}$$

The surface impedance dyadic $\bar{\bar{\boldsymbol{\zeta}}}_\mathrm{r}'$ is symmetric and positive definite; it can be expressed as $\bar{\bar{\boldsymbol{\zeta}}}_\mathrm{r}' = \bar{\mathbf{u}}_x \bar{\mathbf{u}}_x \zeta_x' + \bar{\mathbf{u}}_y \bar{\mathbf{u}}_y \zeta_y'$ without loss of generality. In addition, $\bar{\boldsymbol{\rho}}' = \bar{\mathbf{u}}_x x' + \bar{\mathbf{u}}_y y'$ is the transverse position vector, and subscript 't' denotes 'transverse' with respect to z. Quantity $\bar{\boldsymbol{\Psi}}_\mathrm{s}'(\bar{\boldsymbol{\rho}}')$ is *the electric surface flux density.* The surface normal $\bar{\mathbf{n}}'$ of the anisotropic boundary of the isotropic case coincides with $\bar{\mathbf{u}}_z$.

Because $\bar{\boldsymbol{\rho}}'$, ∇_t', and $\bar{\mathbf{E}}_\mathrm{t}'$ transform as $\bar{\mathbf{r}}'$, ∇', and $\bar{\mathbf{E}}'$, respectively, the boundary condition (D36) transforms as

$$\begin{aligned} & \bar{\mathbf{n}}' \cdot \bar{\mathbf{D}}'(\bar{\boldsymbol{\rho}}') = -\epsilon_0 \nabla_\mathrm{t}' \cdot \bar{\bar{\boldsymbol{\zeta}}}_\mathrm{r}' \cdot \bar{\mathbf{E}}_\mathrm{t}'(\bar{\boldsymbol{\rho}}') \\ \Leftrightarrow \quad & \bar{\mathbf{n}}' \cdot (\epsilon_0 \bar{\bar{\epsilon}}_\mathrm{r}^{1/2} \cdot \bar{\mathbf{E}}_\mathrm{t}(\bar{\boldsymbol{\rho}})) = -\epsilon_0 (\bar{\bar{\epsilon}}_\mathrm{r}^{1/2} \cdot \nabla_\mathrm{t}) \cdot \bar{\bar{\boldsymbol{\zeta}}}_\mathrm{r}' \cdot (\bar{\bar{\epsilon}}_\mathrm{r}^{1/2} \cdot \bar{\mathbf{E}}_\mathrm{t}(\bar{\boldsymbol{\rho}})) \\ \Leftrightarrow \quad & (\bar{\mathbf{n}}' \cdot \bar{\bar{\epsilon}}_\mathrm{r}^{-1/2}) \cdot (\epsilon_0 \bar{\bar{\epsilon}}_\mathrm{r} \cdot \bar{\mathbf{E}}_\mathrm{t}(\bar{\boldsymbol{\rho}})) = -\epsilon_0 \nabla_\mathrm{t} \cdot (\bar{\bar{\epsilon}}_\mathrm{r}^{1/2} \cdot \bar{\bar{\boldsymbol{\zeta}}}_\mathrm{r}' \cdot \bar{\bar{\epsilon}}_\mathrm{r}^{1/2}) \cdot \bar{\mathbf{E}}_\mathrm{t}(\bar{\boldsymbol{\rho}}) \\ \Leftrightarrow \quad & \bar{\mathbf{n}} \cdot \bar{\mathbf{D}}(\bar{\boldsymbol{\rho}}) = -\epsilon_0 \nabla_\mathrm{t} \cdot \bar{\bar{\boldsymbol{\zeta}}}_\mathrm{r} \cdot \bar{\mathbf{E}}_\mathrm{t}(\bar{\boldsymbol{\rho}}). \end{aligned} \tag{D37}$$

We have required $|\bar{\mathbf{n}}| = 1$, and can thus identify

$$\bar{\boldsymbol{\rho}} = \bar{\bar{\boldsymbol{\epsilon}}}_{\mathrm{r}}^{1/2} \cdot \bar{\boldsymbol{\rho}}' \quad \leftrightarrow \quad \bar{\boldsymbol{\rho}}' = \bar{\bar{\boldsymbol{\epsilon}}}_{\mathrm{r}}^{-1/2} \cdot \bar{\boldsymbol{\rho}}\,, \tag{D38}$$

$$\bar{\mathbf{n}} = \frac{\bar{\bar{\boldsymbol{\epsilon}}}_{\mathrm{r}}^{-1/2} \cdot \bar{\mathbf{n}}'}{\sqrt{\bar{\mathbf{n}}' \cdot \bar{\bar{\boldsymbol{\epsilon}}}_{\mathrm{r}}^{-1} \cdot \bar{\mathbf{n}}'}} = \frac{\bar{\bar{\boldsymbol{\epsilon}}}_{\mathrm{r}}^{-1/2} \cdot \bar{\mathbf{u}}_z}{\sqrt{\bar{\mathbf{u}}_z \cdot \bar{\bar{\boldsymbol{\epsilon}}}_{\mathrm{r}}^{-1} \cdot \bar{\mathbf{u}}_z}} \quad \leftrightarrow \quad \bar{\mathbf{n}}' = \frac{\bar{\bar{\boldsymbol{\epsilon}}}_{\mathrm{r}}^{1/2} \cdot \bar{\mathbf{n}}}{\sqrt{\bar{\mathbf{n}} \cdot \bar{\bar{\boldsymbol{\epsilon}}}_{\mathrm{r}} \cdot \bar{\mathbf{n}}}}\,, \quad \text{and} \tag{D39}$$

$$\bar{\bar{\boldsymbol{\zeta}}}_{\mathrm{r}} = \frac{\bar{\bar{\boldsymbol{\epsilon}}}_{\mathrm{r}}^{1/2} \cdot \bar{\bar{\boldsymbol{\zeta}}}_{\mathrm{r}}' \cdot \bar{\bar{\boldsymbol{\epsilon}}}_{\mathrm{r}}^{1/2}}{\sqrt{\bar{\mathbf{n}}' \cdot \bar{\bar{\boldsymbol{\epsilon}}}_{\mathrm{r}}^{-1} \cdot \bar{\mathbf{n}}'}} = \frac{\bar{\bar{\boldsymbol{\epsilon}}}_{\mathrm{r}}^{1/2} \cdot \bar{\bar{\boldsymbol{\zeta}}}_{\mathrm{r}}' \cdot \bar{\bar{\boldsymbol{\epsilon}}}_{\mathrm{r}}^{1/2}}{\sqrt{\bar{\mathbf{u}}_z \cdot \bar{\bar{\boldsymbol{\epsilon}}}_{\mathrm{r}}^{-1} \cdot \bar{\mathbf{u}}_z}} \quad \leftrightarrow \quad \bar{\bar{\boldsymbol{\zeta}}}_{\mathrm{r}}' = \frac{\bar{\bar{\boldsymbol{\epsilon}}}_{\mathrm{r}}^{-1/2} \cdot \bar{\bar{\boldsymbol{\zeta}}}_{\mathrm{r}} \cdot \bar{\bar{\boldsymbol{\epsilon}}}_{\mathrm{r}}^{-1/2}}{\sqrt{\bar{\mathbf{n}} \cdot \bar{\bar{\boldsymbol{\epsilon}}}_{\mathrm{r}} \cdot \bar{\mathbf{n}}}}\,. \tag{D40}$$

As the transforming of $\bar{\mathbf{n}}'$ to $\bar{\mathbf{n}}$ suggests, the anisotropic surface of the anisotropic case, in general, becomes slanted with respect to the anisotropic surface of the isotropic case (the surfaces are defined as $\bar{\mathbf{n}} \cdot \bar{\mathbf{r}} = 0$ and $\bar{\mathbf{n}}' \cdot \bar{\mathbf{r}}' = 0$, respectively). We could use $\bar{\mathbf{n}}$ and, for example, the transformation of $\bar{\mathbf{u}}_x$ to define (after some steps) a coordinate system local to the unprimed system, similar to the Cartesian coordinate system of the isotropic case.

Finally we construct the very simple transformation of sources by using the invariance of charges:

$$\varrho'(\bar{\mathbf{r}}') = \varrho(\bar{\mathbf{r}}) = \varrho(\bar{\bar{\boldsymbol{\epsilon}}}_{\mathrm{r}}^{1/2} \cdot \bar{\mathbf{r}}') = \varrho'(\bar{\bar{\boldsymbol{\epsilon}}}_{\mathrm{r}}^{-1/2} \cdot \bar{\mathbf{r}}). \tag{D41}$$

As stated earlier, we consider the case of a point charge in the isotropic space. Our charge density is therefore $\varrho'(\bar{\mathbf{r}}') = Q'\delta(\bar{\boldsymbol{\rho}}')\delta(z - z_0') = Q'\delta(\bar{\mathbf{r}}' - \bar{\mathbf{r}}_0')$, i.e. we have a charge Q' in $\bar{\mathbf{r}}_0' = \bar{\mathbf{u}}_z z_0'$ ($z_0' > 0$). Applying (D41), we get for the anisotropic space

$$\varrho'(\bar{\mathbf{r}}') = Q'\delta(\bar{\bar{\boldsymbol{\epsilon}}}_{\mathrm{r}}^{-1/2} \cdot \bar{\mathbf{r}} - \bar{\mathbf{u}}_z z_0') = Q'\delta\big(\bar{\bar{\boldsymbol{\epsilon}}}_{\mathrm{r}}^{-1/2} \cdot (\bar{\mathbf{r}} - \bar{\bar{\boldsymbol{\epsilon}}}_{\mathrm{r}}^{1/2} \cdot \bar{\mathbf{u}}_z z_0')\big) = Q\delta(\bar{\mathbf{r}} - \bar{\mathbf{r}}_0) = \varrho(\bar{\mathbf{r}}) \tag{D42}$$

with

$$Q = Q'/\sqrt{\det(\bar{\bar{\boldsymbol{\epsilon}}}_{\mathrm{r}}^{-1/2})} \quad \leftrightarrow \quad Q' = Q/\sqrt{\det(\bar{\bar{\boldsymbol{\epsilon}}}_{\mathrm{r}}^{1/2})}, \tag{D43}$$

$$\bar{\mathbf{r}}_0 = \bar{\bar{\boldsymbol{\epsilon}}}_{\mathrm{r}}^{1/2} \cdot \bar{\mathbf{r}}_0' = \left(\bar{\bar{\boldsymbol{\epsilon}}}_{\mathrm{r}} \cdot \bar{\mathbf{n}}\sqrt{\bar{\mathbf{u}}_z \cdot \bar{\bar{\boldsymbol{\epsilon}}}_{\mathrm{r}}^{-1} \cdot \bar{\mathbf{u}}_z}\right) z_0' \quad \leftrightarrow \quad \bar{\mathbf{r}}_0' = \bar{\bar{\boldsymbol{\epsilon}}}_{\mathrm{r}}^{-1/2} \cdot \bar{\mathbf{r}}_0. \tag{D44}$$

The delta function has been simplified with $\delta(\bar{\bar{\mathbf{A}}} \cdot \bar{\mathbf{r}}) = \delta(\bar{\mathbf{r}})/\det \bar{\bar{\mathbf{A}}}$, which holds for symmetric positive definite dyadics. Transformation of the reflection image $\varrho^{\mathrm{r}\prime}(\bar{\mathbf{r}}')$ in the isotropic space to an image in the anisotropic space is

$$\varrho^{\mathrm{r}}(\bar{\mathbf{r}}) = \varrho^{\mathrm{r}\prime}(\bar{\mathbf{r}}') = \varrho^{\mathrm{r}\prime}(\bar{\bar{\boldsymbol{\epsilon}}}_{\mathrm{r}}^{-1/2} \cdot \bar{\mathbf{r}}). \tag{D45}$$

This step completes our dictionary; constructing the expression of the transformed reflection image would become next, but we end the demonstration of the technique here. The affine transformation has been used, for example, in [D5].

3.3 Kelvin inversion

This is another method for changing the geometry. In paper [P2] Kelvin inversion is used to determine image sources by inverting the outside of a sphere inside it. It would also be possible to use a suitable chosen inversion sphere with respect to a wedge and obtain images sources for a whole new class of geometries [D6].

4 Equivalent sources

The form of the Maxwell equations suggests that if we know the fields everywhere, we also know the sources everywhere. But if we limit our scope only to a volume V, there may be

other sources which give the same fields in V. These sources will be called *equivalent sources* (with respect to V), [D1, p. 165].

We start with a space with some obstacles (or interfaces or scatterers, as they might be called) in it. We can solve for the radiation (statics included) of the original source in a space without the interfaces, then find a suitable equivalent source (a combination of the original source and an auxiliary source) satisfying the boundary conditions, and finally calculate the fields from these two sources in the proper part of the again interfaceless (homogeneous) space. If the auxiliary source somehow resembles a geometric image of the original source, we would call it *the image source,* and the field arising from it *the reflected field.* The uniqueness of the solutions of Maxwell equations (augmented with suitable boundary or radiation conditions) guarantees us the right answer (for a thorough discussion see Section 3.5 of [D1]).

The classical example of the use of an image method is the problem of a point charge Q at height h above an infinite PEC plane. The reflected field at the upper half-space is obtained directly from the image source $-Q$ at height h below the level of the PEC plane after the PEC plane has been removed, and the lower half-space has been filled with the medium of the upper half-space. A homogeneous-space Green function is needed to determine the fields of the image source—the difficult task of finding the geometry-matched Green function is avoided.

The Huygens' principle is another, yet slightly different, example of equivalent sources. In it the original sources are discarded altogether after the equivalent sources on a predefined surface have been obtained; fields inside the surface are solely determined by these sources. For an elegant derivation of the Huygens' principle see [D7].—Multipole expansions representing arbitrary sources also belong to the class of equivalent sources.

It should be noted that if we subtract the field of the equivalent source from the field of the original source, we naturally get zero field in V. The sum of the original source with the negative equivalent source is called *a nonradiating source* with respect to V.

Unfortunately finding equivalent sources is not always possible. For example, the image principle has so far been only used for some simple interface geometries like the plane (static or time-harmonic case) or sphere (static case). On the other hand, when the image is available, it is an intuitively appealing expression of the solution, and mental pictures of difficult problems can be acquired with the aid of it. Some numerical difficulties can also be avoided; see, e.g., the discussion about the exact image theory (EIT) solution [D8] of the Sommerfeld half-space problem.

5 Commentary of Papers [P1]–[P7]

5.1 Paper [P1]

> Oksanen, M.I., Hänninen, J. & Tretyakov, S.A. "Vector circuit method for calculating reflection and transmission of electromagnetic waves in multilayer chiral structures". *IEE Proceedings H, Microwaves, Antennas and Propagation,* **138**(1991)6, p. 513–520.

This paper is the oldest one and is therefore presented first. Also, the frequency range of the method is unlimited (as long as $\omega > 0$); at the later papers we deal with low frequencies or even with statics.

The article is a generalisation of another paper [1],[1] in which the vector circuit method

[1]In Section 5 all references are to the paper in question, unless otherwise noted.

(VCM) was applied to one chiral slab. Now several slabs are stacked upon each other and the reflection and transmission dyadics for the whole structure are determined. The benefit of using dyadic algebra is clear: both eigenpolarisations can be handled simultaneously, and the results have a compact representation.

The setup of the problem is shown in Fig. 1. Tangential components are naturally taken along the planar interfaces. By the "upper side" of the slab is actually meant the left side, and by the "lower side" the right side.

In addition to an equivalence in the solution process (the VCM), we have here an extremely simple equivalent source: it is just two times the tangential component of the electric field of the incoming plane wave and is interpreted as a vector voltage source for the vector transmission line. The impedances of the transmission line sections are dyadics, and the two-port circuit has dyadic transfer parameters. The expressions for the elements of the matrix $[\bar{\bar{\mathbf{a}}}]$ are given in equations (8)–(11) for one slab and in equations (19)–(22) for the combination of the two rightmost slabs; the total $[\bar{\bar{\mathbf{a}}}]$-matrix is obtained by recursively applying equations (19)–(22) to all slabs. Equation (25) gives the input impedance $\bar{\bar{\mathbf{Z}}}_{\mathrm{eq}}$ of the whole structure. The $\bar{\bar{\mathbf{a}}}$, $\bar{\bar{\mathbf{Z}}}_{\mathrm{c}}$, and $\bar{\bar{\mathbf{Z}}}'_{\mathrm{c}}$ dyadics were derived by using a two-dimensional spatial Fourier transformation on the plane of the slabs.

The reflection ($\bar{\bar{\mathbf{R}}}_{\mathrm{e}}$) and transmission ($\bar{\bar{\mathbf{T}}}_{\mathrm{e}}$) dyadics for the tangential electric fields are given by equations (30)–(32). The total reflected and transmitted electric fields for a TE incident wave are given in equations (39) and (40) and for a TM incident wave in equations (43) and (44). The reflection and transmission dyadics contain information about both the co- and cross-polarisation behaviour of the incident wave. The analytical part and all necessary formulas are ready by the end of Section 4.

Since the publication of this paper the research of chirality has produced new theoretical and experimental results (see, e.g. [D9, D10, D11]); chiral materials have been seen to be less superior than they once were thought to be. The physical realizability of the κ-parameters of this article should perhaps be checked one day—if not for the sake of science, then at least for the personal interest.

5.2 Paper [P2]

Lindell, I.V. & Hänninen, J.J. "Static image principle for the sphere in isotropic or bi-isotropic space". *Radio Science,* **35**(2000)3, p. 653–660.

The image principle for a PEC sphere and a (static) electric point charge near the sphere is usually presented on the elementary electromagnetics courses. The equivalent source can be obtained with geometrical reasoning, but in this paper a more formal approach is used. It is good to start the reading of the paper from the Appendix, in which the Kelvin inversion of the Poisson equation and its solution are shown.

First a grounded PEC sphere is located in a dielectric medium, and we get the traditional image charge (7) very easily. Next, a PMC sphere in a dielectric medium is studied, and the method for finding the solution of this problem gives us a guideline for the general case. We first try to use a negative Kelvin image, but we immediately see that it is not enough—the proper boundary condition $\partial_r \phi(\bar{\mathbf{r}})|_{r=a} = 0$ is not satisfied. The correct solution (image source) consists of the Kelvin-inverted original source *and* an augmenting source term corresponding to an additional potential term needed for satisfying the boundary condition. The image of a point charge outside the PMC sphere will be a point charge inside the sphere with a constant line charge connecting the point charge and the centre of the sphere.

The following steps are obvious. A general impedance boundary (16) is studied, and again the image consists of an augmented Kelvin image—the differential operator just gets more complicated. The PEC and PMC spheres are special cases of the general impedance boundary. However, we do not get an expression for a general interface condition ("material sphere"): the Kelvin inversion is not applicable. The material sphere was studied in *Lindell* [1992].

Section 3 generalises the theory even further. The PEC, PMC and impedance spheres are studied each in turn, but they are now embedded in a bi-isotropic medium (the chiral medium being one special case). The existence of bi-isotropy requires time-harmonic fields, but we may assume that the frequency is low and approach the situation in a quasi-static sense. This means that the wavelength inside the sphere has to be much larger than the diameter of the sphere.

The notation here is a mixed matrix–vector notation, or six-vector notation. The calculations are a bit longer, but not overwhelming. Because the electric and magnetic fields become coupled in a bi-isotropic medium, the images of electric charges will consist of electric *and* magnetic charges. The final image (49) collects all cases—PEC, PMC and impedance spheres in dielectric or bi-isotropic medium.

5.3 Paper [P3]

> Lindell, I.V., Hänninen, J.J. & Pirjola, R. "Wait's complex-image principle generalized to arbitrary sources". *IEEE Transactions on Antennas and Propagation,* **48**(2000)10, p. 1618–1624.

This paper and [P4] concentrate on finding and applying image sources in a straightforward manner.

The Geophysical Research Division of the Finnish Meteorological Institute has a long history in the research of space weather and geoelectromagnetics (see the references of [P4]). Papers [P3] and [P4] are the first results of the co-operation of FMI/GEO and the HUT Electromagnetics Laboratory on this subject.

"Wait's image principle" refers to the complex image principle which J.R. Wait introduced in 1969 [1]–[3]. It is valid for horizontal divergenceless currents at low frequencies. These limitations were removed with the exact image theory (EIT) in 1984 [5]. Wait's theory has been very useful in geoelectromagnetics because it is simple and makes fast computations possible.

The EIT is a general method for handling reflection and transmission of electromagnetic waves in conjunction with planar interfaces. The main differences with Wait's theory are that the EIT is valid for any current distribution at all frequencies and that the image of a point source is a line current in complex space—in Wait's theory the image of a point source is a point source at a complex depth. As in all image theories, the equivalent source (of the total field) is the combination of the image source and the original source. Calculation of the fields on different sides of the interface requires different image sources (reflection and transmission images).

Section II of the paper introduces the basic formulas of the exact image theory, first in general form and then for a (horizontally) planar current density. The image current is obtained by operating to the original current with the reflection transformation $\bar{\bar{\mathbf{C}}}$ and with a dyadic operator containing the image functions $f^{\mathrm{TE}}(\zeta)$, $f^{\mathrm{TM}}(\zeta)$, and $f_0(\zeta)$ of the complex integration parameter ζ (equation (7)). The image functions, in turn, depend on the two-parameter function $f(\alpha, p)$, which is an infinite sum of Bessel functions when $\alpha \neq 1$

(eq. (13)). Low-frequency approximations of the exact image current are available via the proper approximation of $f(\alpha, p)$.

Part B of Section II contains the first approximations. The sum of the Bessel functions is rewritten in form (14) for very large values of $|\alpha|$. In geophysics the ground is assumed nonmagnetic, $\mu_r = 1$. Because the frequency is low and the ground is conductive, the imaginary part of the complex permittivity will be large, i.e. $|\epsilon_r|$ is large. So, in some image functions—those containing the permittivity of the ground—$|\alpha|$ will be large.

When the $g(p)$-formulation of (14) is combined with the final forms of equations (15) and (16), we get what will be called 'asymptotically accurate' approximation of $f(\alpha, p)$ and thus of the image current.

The derivation of the 'delta-function approximation' of $f(\alpha, p)$ starts with the application of the identities (17) to equation (12). Then the moment integrals of type (18) are computed with the first two terms of the delta-function expansion of $f(\alpha, p)$ as their integrands. Finally, comparison of the integration results gives us the approximation (19).

Section III utilises the obtained approximations in the image functions. The asymptotic form of $f^{\mathrm{TE}}(\zeta)$ can be chosen to be the same as the exact form because the exact function is very simple. The two other image functions are presented in the $g(p)$-approximated forms.

It is nice to see that the delta-approximated image function $f^{\mathrm{TE}}(\zeta)$ in part B gives the Wait image (27). To get the delta-approximations of the two remaining functions, the step-function-like $g(p)$ has to be approximated once more. After the calculations (28)–(30) we are able to write an extension to the Wait image, equations (31) and (33).

In Section IV the approximated image functions are used in examples of image currents. The cases of a vertical dipole, horizontal dipole, and a point charge (though it is non-physical) are covered. Section V, in turn, contains a numerical example which is actually extracted from paper [P4].

5.4 Paper [P4]

> Hänninen, J.J., Pirjola, R.J. & Lindell, I.V. "Application of the EIT to studies of ground effects of space weather". *Geophysical Journal International,* **151**(2002)-, p. 534–542.

Space weather is a result of the activity of the Sun. The solar wind (a flux of charged particles) causes currents in the ionosphere of the Earth, and these in turn radiate electromagnetic fields, which then reflect from the ground. The total field—the sum of the incoming and reflected fields—induces currents in technological systems at the surface of the Earth, e.g. in electric transmission lines and gas pipelines, causing disturbances and even damage. The aim of space weather research is to develop methods for predicting and understanding the geomagnetically induced currents (GICs). For this purpose we need to know the tangential electric fields at the surface of the earth.

In this paper a very crude geophysical current model is considered. The chosen model is a wave-like line current above a conducting half-space. An actual ionospheric current cannot be of this form because the high conductivity of the ionosphere prevents accumulation of charges. Anyway, this model is a good test for the applicability of the EIT to this kind of problems. The principles of the exact image theory were presented in the commentary of paper [P3], so we can concentrate on the test result.

Paper [P3] told only the general principles for calculating the fields from a current source. Section 3 of [P4], in turn, contains detailed formulas for determining the vector potential of a line current. It also has preliminary formulas for the related electric field strength and

magnetic flux density. In Section 4 the incident electric and magnetic fields are computed, and in Section 5 the approximate image functions are finally applied to the reflected fields. Both the asymptotically accurate and the delta-function approximated field expressions are shown. The calculations of Sections 4 and 5 are straightforward but elaborate, and the resulting field expressions are long.

The practical aspects of applying equivalent sources come into play here. Because the Green function (10) includes a complex distance function $\sqrt{\bar{\mathbf{r}} \cdot \bar{\mathbf{r}}}$ (the position vector $\bar{\mathbf{r}}$ is complex), we have to select the correct branch for the square root, which is not a trivial task—the position vector $\bar{\mathbf{r}}$ itself contains a square root of the complex number B! There are four sign combinations, and only one of them gives physically meaningful results. The selection of the proper branch cut was partly carried out by trial and error, and partly by some (yet unpublished) selection rules.

The numerical results are promising, especially those using the asymptotically accurate image. The delta-function approximation does not always work that well, and the reason is clear: we are trying to get an almost zero tangential electric field at the surface of the earth by subtracting two large numbers, so small relative errors in the reflected fields show up in the total fields. Nevertheless, the reflected fields themselves are very good-looking. Obviously the EIT-given approximations are applicable in future work; a good approximation for the *total field* would, of course, be a worthy goal.

5.5 Paper [P5]

> Lindell, I.V., Hänninen, J.J. & Nikoskinen, K.I. "Electrostatic image theory for an anisotropic boundary". *IEE Proceedings—Science, Measurement & Technology,* accepted for publication.

We now return to electrostatics (or, via a change of symbols, to steady-current problems). Here we have an isotropic half-space bounded by an anisotropic impedance boundary. A boundary of this type can be obtained by letting the thickness of a PMC-backed slab of anisotropic permittivity approach zero while the permittivity approaches infinity so that the thickness–permittivity product remains finite (see [D12]). The boundary condition will take form (8).

This paper uses the transmission line analogy described in Section 3.1. The Fourier transformation (1) is applied to all quantities, and after some algebraic work-out the transmission line equations appear. In (29) the reflection sources are expressed as functions of the reflection operator and the $z = 0$-reflected original sources.

The reflection coefficient is a function of the transmission line impedance (23) and terminating impedance (24). It is turned into an operator through the equivalence $K^n e^{-Kz} = (-\partial_z)^n e^{-Kz}$. The reflection image source is obtained by carrying out the inverse Fourier transformation symbolically, (31), which gives us the operational form of the image, (35). This is interpreted as a Klein–Gordon type differential equation, finally leading to the quasi-physical image (46), (47). The image source consists of two parts: of a point source on the mirror image point and of a sector of a vertical surface charge having line charges (delta functions) on its edges.—The operators here are an example of the *Heaviside operator calculus*, see e.g. [D13]. We already met the operator calculus in conjunction with paper [P2].

Section 5 of the paper presents some additional forms of the image (equivalence forms of an equivalent source...), and in Section 6 the results are compared with earlier theories; a good agreement is seen. A numerical test is described in Section 7, its outcome also being very satisfactory.

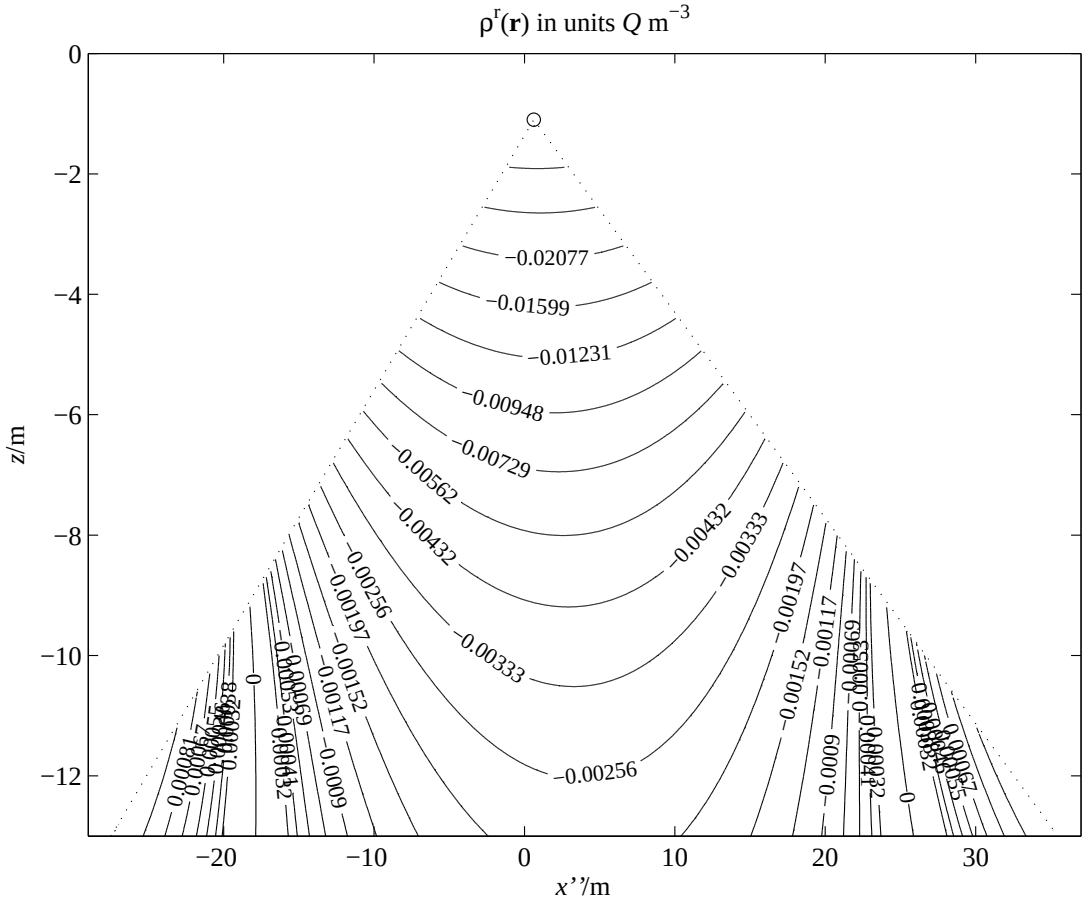

Figure D2: Equicharge contours in the $x''z$-plane for the case discussed in Section 5.6. The circle denotes the shifted mirror image position.

5.6 Paper [P6]

Hänninen, J.J., Lindell, I.V. & Nikoskinen, K.I. "Electrostatic image theory for an anisotropic boundary of an anisotropic half-space". *Progress in Electromagnetics Research,* **47**(2004)-, p. 235–262.

The principal similarity of papers [P5]–[P7] makes it unnecessary to repeat all the details of the formulation. Of course, because [P6] and [P7] deal with an anisotropic half-space above an anisotropic surface impedance or half-space, respectively, something new has to appear, and it is the two-dimensional dyadic $\overline{\overline{\mathbf{T}}}$. Constructing the transmission line equations is helped by the existence of $\overline{\overline{\mathbf{T}}}$, inside which the details of the upper half-space medium are swept. Another significant innovation is the "shifting vector" $\bar{\mathbf{a}}$. In Section 4 the square root of $\overline{\overline{\mathbf{T}}}$ is used twice to turn the anisotropic problem into an isotropic one (by an affine transformation, actually), after which the known results of paper [P5] give us the solution of this problem. The obtained image function is just a shifted, skewed, and slanted version of the one in [P5].

The anisotropic permittivity dyadic $\overline{\overline{\boldsymbol{\epsilon}}}_{\mathrm{r}}$ is the most general possible in electrostatics, i.e. it is symmetric and positive definite. As is evident from the paper, these two properties are heavily utilised in the solution process. The surface impedance dyadic $\overline{\overline{\boldsymbol{\zeta}}}_{\mathrm{r}}$ possesses the same generality features.

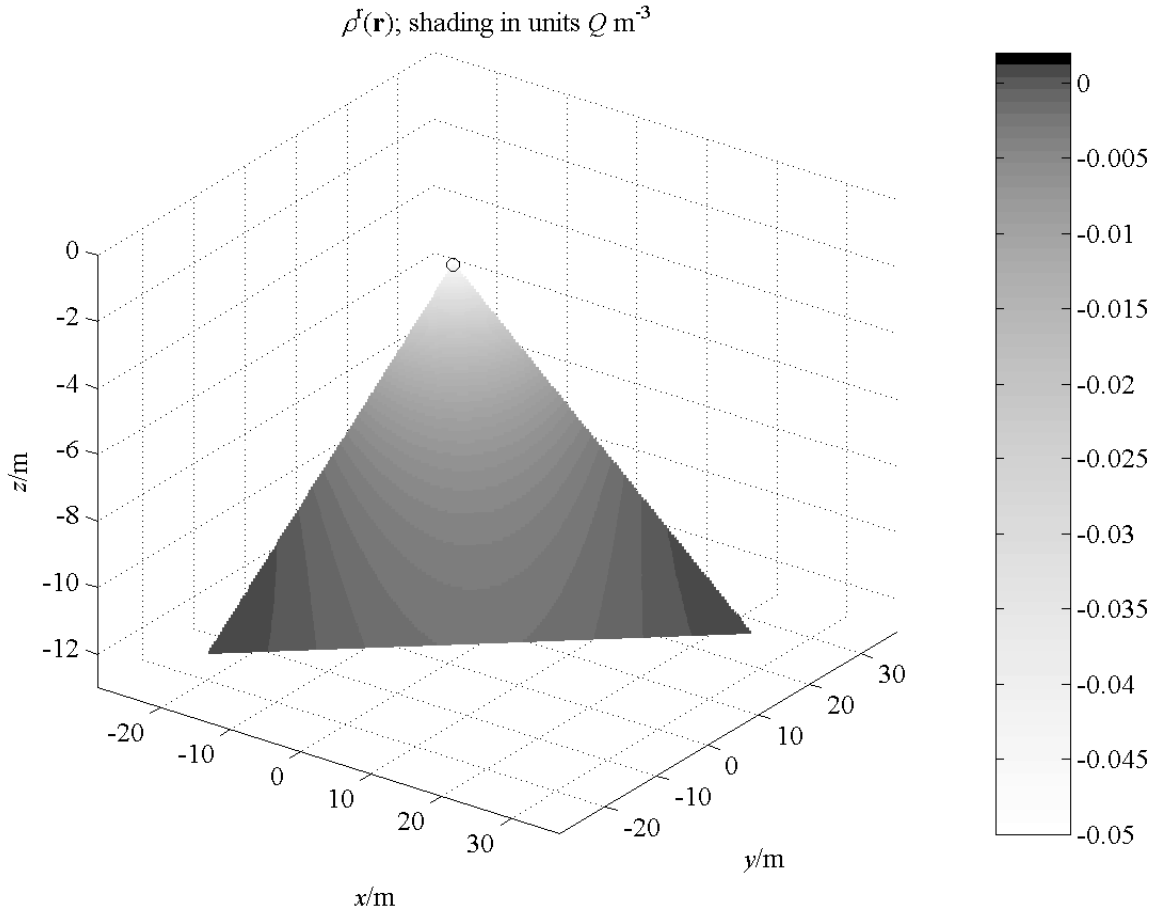

Figure D3: Charge distribution of the planar image source of Section 5.6. The true orientation of the source is shown. Again the circle is in the location of the point source.

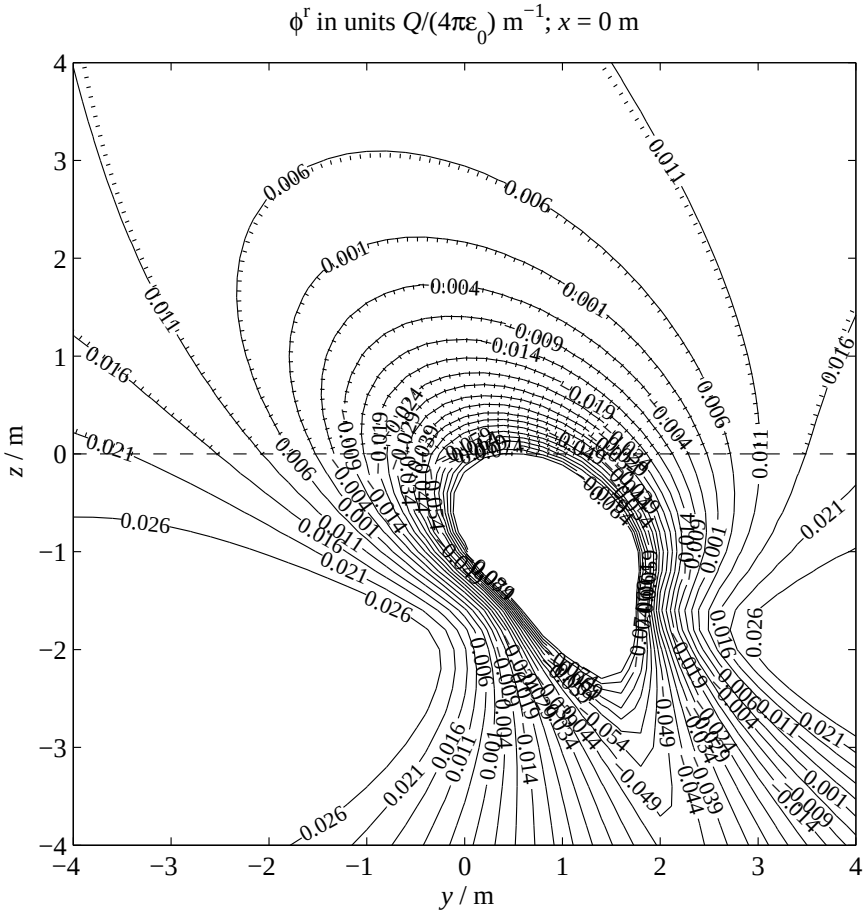

Figure D4: Equipotential contours in the $x = 0$ m plane for the reflection problem of Section 5.6.

There are no potential figures in paper [P6], but that is mended here. We have chosen as the medium parameters—in close resemblance to [P7]—

$$\bar{\bar{\epsilon}}_{\mathrm{r}} = \bar{\mathbf{u}}_x\bar{\mathbf{u}}_x 8 + \bar{\mathbf{u}}_y\bar{\mathbf{u}}_y 19/8 - (\bar{\mathbf{u}}_y\bar{\mathbf{u}}_z + \bar{\mathbf{u}}_z\bar{\mathbf{u}}_y)\sqrt{3}/2 + \bar{\mathbf{u}}_z\bar{\mathbf{u}}_z 2,$$

$$\bar{\bar{\bar{\zeta}}}_{\mathrm{r}} = \bar{\mathbf{u}}_x\bar{\mathbf{u}}_x 32 + (\bar{\mathbf{u}}_x\bar{\mathbf{u}}_y + \bar{\mathbf{u}}_y\bar{\mathbf{u}}_x)8\sqrt{3} + \bar{\mathbf{u}}_y\bar{\mathbf{u}}_y 16, \quad \text{and} \quad z_0 = 1.1 \text{ m}, \tag{D46}$$

giving us the computed parameters

$$\bar{\mathbf{a}} = -\bar{\mathbf{u}}_y\sqrt{3}/4, \quad \zeta'_y = 2, \quad \text{and} \quad \zeta''_{\mathrm{d}} = 14. \tag{D47}$$

The image charge distribution (excluding the edge charges) is presented in Figures (D2) and (D3). The normalised equipotential curves are shown in Figures (D4)–(D6). The agreement between the image theory results (solid lines) and inverse FFT comparison result (dotted lines) is clearly seen. The large curve-free voids in the lower half-space are due to selecting the limited set of equipotential values from Figure (D6). The lower half-space curves are not physically valid in the sense of the original problem.

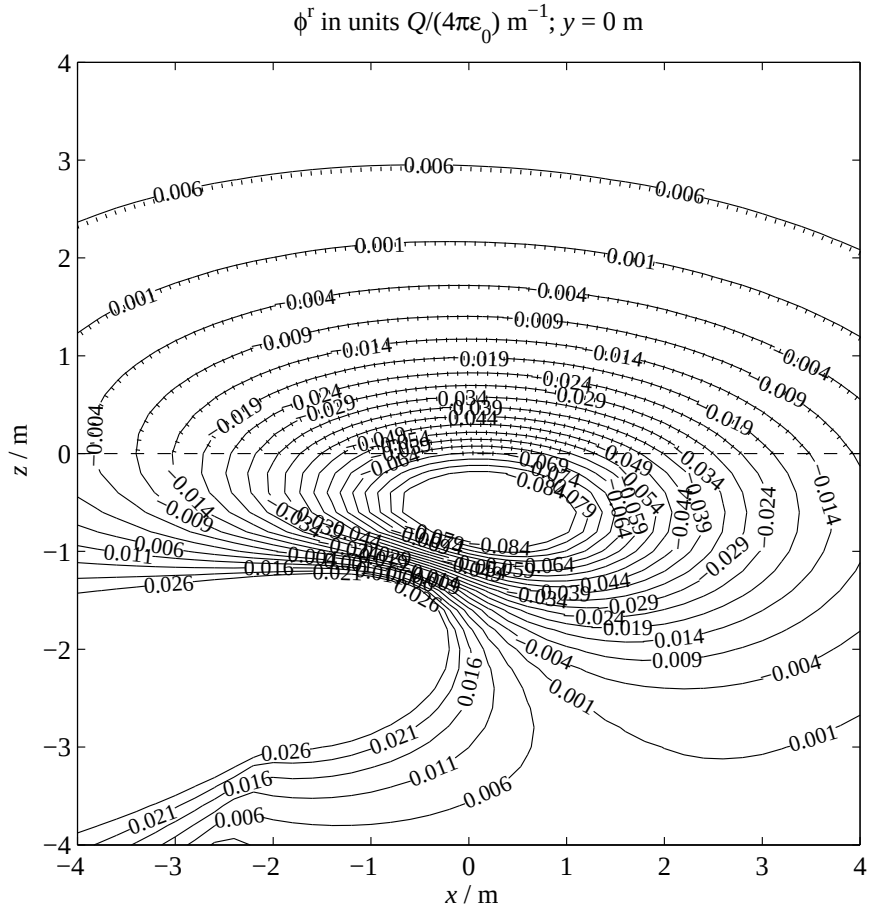

Figure D5: Equipotential contours in the $y = 0$ m plane for the anisotropic problem of Section 5.6.

A note on the numerical computations

We start with the potential integral (71), substitute the image source (70) into it (a superscript circle denotes source region), and integrate by parts:

$$
\begin{aligned}
\frac{4\pi\epsilon_0\phi^{\mathrm{r}}(\bar{\mathbf{r}})}{Q} =& \frac{1}{\sqrt{\det\bar{\bar{\boldsymbol{\epsilon}}}_{\mathrm{r}}}}\int_{-\infty}^{\infty}\int_{-\infty}^{\infty}\int_{-\infty}^{\infty}\Bigg\{ -\delta(\bar{\mathbf{r}}^{\circ}+\bar{\mathbf{s}}+\bar{\mathbf{u}}_z z_0) - \frac{1}{\sqrt{\zeta_y'\zeta_{\mathrm{d}}''}}\delta(y''^{\circ}+a_y''(z_0-z^{\circ})) \\
&\times (\partial_{z^{\circ}}+a_x''\partial_{x''^{\circ}})\Bigg[\exp\!\left(\frac{z^{\circ}+z_0}{2\zeta_y'}\right) I_0\!\left(\sqrt{\frac{(z^{\circ}+z_0)^2}{4{\zeta_y'}^2}-\frac{[x''^{\circ}+a_x''(z_0-z^{\circ})]^2}{4\zeta_y'\zeta_{\mathrm{d}}''}}\right) \\
&\times \Theta\!\left(-\sqrt{\zeta_{\mathrm{d}}''/\zeta_y'}(z^{\circ}+z_0)-x''^{\circ}-a_x''(z_0-z^{\circ})\right) \\
&\times \Theta\!\left(-\sqrt{\zeta_{\mathrm{d}}''/\zeta_y'}(z^{\circ}+z_0)+x''^{\circ}+a_x''(z_0-z^{\circ})\right)\Bigg]\Bigg\} \\
&\times \frac{1}{\sqrt{(\bar{\mathbf{r}}-\bar{\mathbf{r}}^{\circ})\cdot\bar{\bar{\boldsymbol{\epsilon}}}_{\mathrm{r}}^{-1}\cdot(\bar{\mathbf{r}}-\bar{\mathbf{r}}^{\circ})}}\,dx''^{\circ}\,dy''^{\circ}\,dz^{\circ} \\
=& \frac{1}{\sqrt{\det\bar{\bar{\boldsymbol{\epsilon}}}_{\mathrm{r}}}}\Bigg\{\frac{-1}{\sqrt{(\bar{\mathbf{r}}+\bar{\mathbf{s}}+\bar{\mathbf{u}}_z z_0)\cdot\bar{\bar{\boldsymbol{\epsilon}}}_{\mathrm{r}}^{-1}\cdot(\bar{\mathbf{r}}+\bar{\mathbf{s}}+\bar{\mathbf{u}}_z z_0)}} + \int_{-\infty}^{\infty}\int_{-\infty}^{\infty}\int_{-\infty}^{\infty}\frac{1}{\sqrt{\zeta_y'\zeta_{\mathrm{d}}''}} \\
&\times \Bigg[\exp\!\left(\frac{z^{\circ}+z_0}{2\zeta_y'}\right) I_0\!\left(\sqrt{\frac{(z^{\circ}+z_0)^2}{4{\zeta_y'}^2}-\frac{[x''^{\circ}+a_x''(z_0-z^{\circ})]^2}{4\zeta_y'\zeta_{\mathrm{d}}''}}\right) \\
&\times \Theta\!\left(-\sqrt{\zeta_{\mathrm{d}}''/\zeta_y'}(z^{\circ}+z_0)-x''^{\circ}-a_x''(z_0-z^{\circ})\right) \\
&\times \Theta\!\left(-\sqrt{\zeta_{\mathrm{d}}''/\zeta_y'}(z^{\circ}+z_0)+x''^{\circ}+a_x''(z_0-z^{\circ})\right)\Bigg] \\
&\times (\partial_{z^{\circ}}+a_x''\partial_{x''^{\circ}})\,\frac{\delta(y''^{\circ}+a_y''(z_0-z^{\circ}))}{\sqrt{(\bar{\mathbf{r}}-\bar{\mathbf{r}}^{\circ})\cdot\bar{\bar{\boldsymbol{\epsilon}}}_{\mathrm{r}}^{-1}\cdot(\bar{\mathbf{r}}-\bar{\mathbf{r}}^{\circ})}}\,dx''^{\circ}\,dy''^{\circ}\,dz^{\circ}\Bigg\} \\
=& \frac{1}{\sqrt{\det\bar{\bar{\boldsymbol{\epsilon}}}_{\mathrm{r}}}}\Bigg\{\frac{-1}{\sqrt{(\bar{\mathbf{r}}+\bar{\mathbf{s}}+\bar{\mathbf{u}}_z z_0)\cdot\bar{\bar{\boldsymbol{\epsilon}}}_{\mathrm{r}}^{-1}\cdot(\bar{\mathbf{r}}+\bar{\mathbf{s}}+\bar{\mathbf{u}}_z z_0)}} \\
&+ \frac{1}{\sqrt{\zeta_y'\zeta_{\mathrm{d}}''}}\int_{-\infty}^{\infty}\int_{-\infty}^{\infty}\exp\!\left(\frac{z^{\circ}+z_0}{2\zeta_y'}\right) I_0\!\left(\sqrt{\frac{(z^{\circ}+z_0)^2}{4{\zeta_y'}^2}-\frac{[x''^{\circ}+a_x''(z_0-z^{\circ})]^2}{4\zeta_y'\zeta_{\mathrm{d}}''}}\right) \\
&\times \Theta\!\left(-\sqrt{\zeta_{\mathrm{d}}''/\zeta_y'}(z^{\circ}+z_0)-x''^{\circ}-a_x''(z_0-z^{\circ})\right) \\
&\times \Theta\!\left(-\sqrt{\zeta_{\mathrm{d}}''/\zeta_y'}(z^{\circ}+z_0)+x''^{\circ}+a_x''(z_0-z^{\circ})\right) \\
&\times \left[\frac{(\bar{\mathbf{a}}+\bar{\mathbf{u}}_z)\cdot\bar{\bar{\boldsymbol{\epsilon}}}_{\mathrm{r}}^{-1}\cdot(\bar{\mathbf{r}}-\bar{\mathbf{r}}^{\circ})}{\left((\bar{\mathbf{r}}-\bar{\mathbf{r}}^{\circ})\cdot\bar{\bar{\boldsymbol{\epsilon}}}_{\mathrm{r}}^{-1}\cdot(\bar{\mathbf{r}}-\bar{\mathbf{r}}^{\circ})\right)^{3/2}}\right]_{y''^{\circ}=-a_y''(z_0-z^{\circ})} dx''^{\circ}\,dz^{\circ}\Bigg\}.
\end{aligned}
\tag{D48}
$$

This is then evaluated numerically. After a substitution of $\sqrt{\zeta_{\mathrm{d}}''/\zeta_y'}(z^{\circ}+z_0)\cos\xi^{\circ}$, $0\le\xi^{\circ}\le\pi$, for $x''^{\circ}+a_x''(z_0-z^{\circ})$, we have integration over a rectangular $\xi^{\circ}z^{\circ}$-region, and the numerical integration behaves much better than with the original sector-like source.

In the numerical calculation of the inverse FFT (see [P7, (77)]) some caution is required too. There is a possibility of division by zero, unless K is canceled from both the numerator (plain K) and the denominator (inside $\gamma_1(\bar{\mathbf{K}})$). The $K\to\infty$ can be taken care of by a suitable change of variables, e.g., by using $\tan\psi$, $0\le\psi\le\pi/2$, for K.

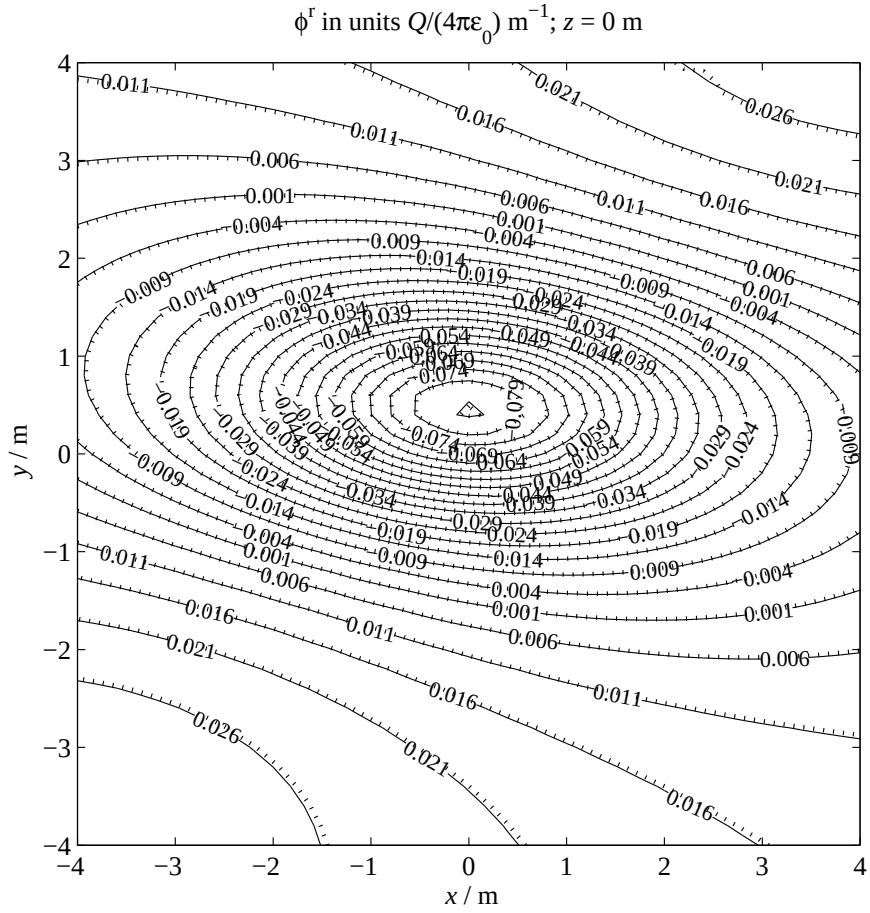

Figure D6: Equipotential contours in the $z = 0$ m plane, see Section 5.6.

5.7 Paper [P7]

Hänninen, J.J., Nikoskinen, K.I. & Lindell, I.V. *Electrostatic image theory for two anisotropic half-spaces.* (Electromagnetics Laboratory Report Series, Report 428). Espoo, Finland 2004: Helsinki University of Technology, Electromagnetics Laboratory. (Submitted in shorter form to *Electrical Engineering (Archiv für Elektrotechnik).*)

The lead-in to the solution of the two-half-space problem is like in [P6] above. Now we just need two permittivity dyadics instead of a permittivity dyadic and a surface impedance dyadic. The positive definiteness and symmetry of the dyadics are assumed. The reflection coefficient will be more symmetric than in the surface case, because the loading impedance has the same form as the line impedance. After finding out the reflection coefficient and making the necessary affine transformations we can use the old theory of [D14].

The shape of the image source is similar to that in [P6], but the charge distribution is of course different. Whereas in [P6] we had a Bessel function, the charge density is now a simpler transcendental function with an integrable singularity (not a delta function!) on its edge.

As the two earlier papers, this one also includes verifications of the validity of the image source, the most remarkable of them being the numerical test. It is highly unlikely to select material parameters which would give so closely coinciding results from two very different computation methods by chance.

6 Conclusion

Several equivalent sources and indirect solution methods in different geometries were presented. Except of paper [P1] all equivalent sources were image sources. The most often used solution-level equivalence method was based on transmission line analogy.

Paper [P2] generalises the static image principle of the sphere to various spheres in isotropic or bi-isotropic media by using the Kelvin inversion. The history of image solutions for spherical geometries is also presented in the paper. The next step would be obtaining a good time-harmonic image theory for the sphere, but the task is very difficult or even impossible to carry out.

Paper [P3] contains the basic approximations suitable for geophysics and [P4] utilises them in a simple example. The planar geometry makes the use of the EIT possible, but getting application-quality results needs further research. The next current model could include a current line with vertical pulsating currents that prevent the accumulation of charges encountered in our example. There is a need for a fast calculation method of the fields at the surface of a layered earth. From the EIT point of view this is a true challenge because the solution of the multilayered problem will be very complicated—the reflection and transmission dyadics would be applied several times. There exists a solution for a slab in an otherwise homogeneous space [D15], but it is not applicable to geophysics as such.

As was mentioned with [P4], the selection of the branches of the square roots in the exact image theory lacks well-established rules. One paper considers the subject [D16], but some questions remain still unanswered. Especially, if we move to the multilayer problem, the choice of the branches will become even more complicated.

Papers [P5]–[P7] give solutions, via the transmission-line model, for some canonical anisotropic problems of electrostatics. These solutions, too, might find use in geophysics—especially if formulated for steady currents. The setting of [P7] could be studied further: there is room for a transmission image source, whose construction will probably be attempted in the near future.

References

[D1] Lindell, I.V. *Methods for Electromagnetic Field Analysis.* 2nd ed. Piscataway, NJ 1995: IEEE Press.

[D2] Dirac, P.A.M. "Quantised singularities in the electromagnetic field". *Proceedings of the Royal Society of London, Series A,* **133**(1931)821, p. 60–72.

[D3] Landau, L.D., Lifshitz, E.M. & Pitaevskiĭ, L.P. *Electrodynamics of Continuous Media.* (Landau and Lifshitz Course of Theoretical Physics; vol 8). 2nd ed. Oxford 1984: Pergamon Press.

[D4] Kong, J.A. *Electromagnetic Wave Theory.* Cambridge, MA 2000: EMW Publishing.

[D5] Lindell, I.V., Ermutlu, M.E., Nikoskinen, K.I. & Eloranta, E.H. "Static image principle for anisotropic conducting half-space problems: impedance boundary". *Geophysics,* 59(1993)12, p. 1773–1778.

[D6] Nikoskinen, K.I. & Hänninen, J. "Kelvin's inversion in wedge geometry". In: Stuchly, M.A. & Shannon D.G., editors. *Proceedings of the 2001 URSI International Symposium on Electromagnetic Theory;* 2001 May 13–17; Victoria, Canada. 2001: URSI. p. 119–121

[D7] Lindell, I.V. "Huygens' principle in electromagnetics". *IEE Proceedings—Science, Measurement & Technology,* **143**(1996)2, p. 103–105.

[D8] Lindell, I.V. & Alanen, E. "Exact image theory for the Sommerfeld half-space problem". *IEEE Transactions on Antennas and Propagation,* **32**(1984) no. 2, p. 126–133, no. 8, p. 841–847, no. 10, p. 1027–1032.

[D9] Ruotanen, L.H. & Hujanen, A. "Simple derivation of the constitutive parameters of an isotropic chiral slab from wideband measurement data". *Microwave and Optical Technology Letters,* **12**(1996)1, p. 40–45.

[D10] Lindell, I.V., Sihvola, A.H., Puska, P. & Ruotanen, L.H. "Conditions for the parameter dyadics of lossless bianisotropic media". *Microwave and Optical Technology Letters,* **8**(1995)5, p. 268–272.

[D11] Ruotanen, L.H. & Hujanen, A. "Experimental verification of physical conditions restricting chiral material parameters". *Journal of Electromagnetic Waves and Applications,* **11**(1997)1, p. 21–35.

[D12] Lindell, I.V. & Nikoskinen, K.I. "Image method for electrostatic problems involving planar anisotropic media based on transmission-line analogy". *Archiv für Elektrotechnik,* **77**(1994)-, p. 251–257.

[D13] Lindell, I.V. "Heaviside operator calculus in electromagnetic image theory". *Journal of Electromagnetic Waves and Applications,* **11**(1997)-, p. 119–132.

[D14] Lindell, I.V., Nikoskinen, K.I. & Viljanen, A. "Electrostatic image method for the anisotropic half-space". *IEE Proceedings—Science, Measurement & Technology,* **144**(1997)4, p. 156–162.

[D15] Lindell, I.V. "Exact image theory for the slab problem". *Journal of Electromagnetic Waves and Applications,* **2**(1988)2, p. 195–215.

[D16] Lindell, I.V. "On the integration of image sources in exact image method of field analysis". *Journal of Electromagnetic Waves and Applications,* **2**(1988)7, p. 607–619.

421. I.V. Lindell, K.H. Wallén: Generalized Q-media and field decomposition in differential-form approach, December 2003.

422. H. Wallén, A. Sihvola: Polarizability of conducting sphere-doublets using series of images, January 2004.

423. A. Sihvola (editor): Electromagnetics Laboratory Annual Report 2003, February 2004.

424. J. Venermo, A. Sihvola: Electric polarizability of circular cylinder, February 2004.

425. A. Sihvola: Metamaterials and depolarization factors, February 2004.

426. T. Uusitupa: Studying electromagnetic wave-guiding and resonating devices, February 2004.

427. I.V. Lindell: Affine transformations and bi-anisotropic media in differential-form approach, March 2004.

428. J.J. Hänninen, K.I. Nikoskinen, I.V. Lindell: Electrostatic image theory for two anisotropic half-spaces, March 2004.

429. M. Norgren, J. Avelin, A. Sihvola: Depolarization dyadic for a cubic cavity: illustrations and interpretation, March 2004.

430. K. Heiska: On the modeling of WCDMA system performance with propagation data, April 2004

431. J. Jylhä, A. Sihvola: Numerical modelling of random media using pseudorandom simulations, April 2004.

432. S. Järvenpää, P. Ylä-Oijala: High order boundary element method for general acoustic boundary value problems, April 2004.

433. P. Ylä-Oijala, M. Taskinen: General CFIE formulation for electromagnetic scattering by composite metallic and dielectric objects.

434. Jari J. Hänninen: Solving electromagnetic boundary problems with equivalence methods, April 2004.

ISBN 951-22-7080-3

ISSN 1456-632X

Picaset Oy, Helsinki 2004